GEOPHYSICS. VOL. 76, NO. 5 (SEPTEMBER-OCTOBER 2011); PP. 1–9, 11 FIGS., 4 TABLES.
10.1190/GEO2010-0258.1

Source-rock seismic-velocity models: Gassmann versus Backus

José M. Carcione[1], Hans B. Helle[2], and Per Avseth[3]

ABSTRACT

Source rocks are described by a porous transversely isotropic medium composed of illite and organic matter (kerogen, oil, and gas). The bulk modulus of the oil/gas mixture is calculated by using a model of patchy saturation. Then, the moduli of the kerogen/fluid mixture are obtained with the Kuster and Toksöz model, assuming that oil is the inclusion in a kerogen matrix. To obtain the seismic velocities of the shale, we used Backus averaging and Gassmann equations generalized to the anisotropic case with a solid-pore infill. In the latter case, the dry-rock elastic constants are calculated with a generalization of Krief equations to the anisotropic case. We considered eleven samples of the Bakken-shale dataset, with a kerogen pore infill. The Backus model provides lower and upper bounds of the velocities, whereas the Krief/Gassmann model provides a good match to the data. Alternatively, we obtain the dry-rock elastic moduli by using the inverse Gassmann equation, instead of using Krief equations. Four cases out of eleven yielded physically unstable results. We also considered samples of the North Sea Kimmeridge shale. In this case, Backus performed as well as the Krief/Gassmann model. If there is gas and oil in the shale, we found that the wave velocities are relatively constant when the amount of kerogen is kept constant. Varying kerogen content implies significant velocity changes versus fluid (oil) saturation.

INTRODUCTION

Hydrocarbons can be extracted from source rocks, particularly shales, for instance, the black shales of the Bakken formation (Vernik and Nur, 1992) and the Kimmeridge shale of the North Sea (Vernik, 1995). The pore space can be filled with kerogen, oil, and gas. These source rocks are characterized by a remarkable velocity anisotropy due to the microlaminated distribution of kerogen and alignment of the clay particles, mainly illite. Therefore, a suitable model describing the wave velocities is essential to quantify the amount of organic matter from seismic data.

Generally, hydrocarbon source rocks can be approximated by transversely isotropic media composed of organic matter and illite layers. Note that this may not be the case for source rocks with low clay content, which mostly have quartz or carbonate. Moreover, some source rocks have kerogen in equant cavities and not in thin layers (Sondergeld et al., 2010). To our knowledge, Vernik and coworkers and Carcione (2000) proposed the only existing models to describe the acoustic properties of source rocks, using Backus averaging. Vernik and Nur (1992) obtained the seismic velocities in a kerogen-rich shale, and Carcione (2000) calculated the excess pore pressure as a function of the fraction of kerogen converted to oil and introduced seismic attenuation. Alternative models were proposed for water-saturated shales. The model of Hornby et al. (1994) is based on a combination of anisotropic formulations of the self-consistent and differential effective-medium approximations. They consider a clay-platelet angular distribution taken from scanning electron microscope (SEM) images that it is used to obtain more realistic elastic constants. Sayers (1999) assumes that the stress dependence of the elastic properties of a shale is due to the deformation of the contact regions between clay platelets. Sarout and Guéguen (2008) developed a micromechanical model to obtain effective elastic properties and anisotropy in terms of its microscopic features, such as intrinsic anisotropy and crack/pore geometry. The model, based on Eshelby theory, considers oblate spheroidal pores aligned in the bedding plane of a transversely isotopic elastic background. Finally, Ciz and Shapiro (2009) proposed a porosity-deformation approach, based on a piezosensitivity theory, to describe elastic moduli of anisotropic shales as nonlinear functions of the effective stress. All these models could, in principle, be modified to introduce the effects of kerogen as a pore-filling material, although this extension is not evident.

Manuscript received by the Editor 11 August 2010; revised manuscript received 18 February 2011.
[1]Istituto Nazionale di Oceanografia e di Geofisica Sperimentale (OGS), Trieste, Italy. E-mail: jcarcione@ogs.trieste.it.
[2]Odin Petroleum, Bergen, Norway.
[3]Odin Petroleum, Bergen, Norway; and Norwegian University of Science and Technology, Trondheim, Norway. E-mail: per.avseth@odin-petroleum.no.

Here, we use Gassmann equations for an anisotropic frame and an isotropic solid-pore infill (kerogen-oil-gas) (Ciz and Shapiro, 2007). The dry-rock elastic constants involved in Gassmann equations are obtained by a generalization of Krief equations to the anisotropic case (see the isotropic version in Krief et al., 1990). By "dry rock," we mean the rock exclusive of pore fill (kerogen, oil, and gas), whereas "wet rock" refers to the rock including the pore fill. Bound water is part of the rock frame and not of the pore fill. The effect of partial saturation on velocity depends on the frequency range (e.g., Avseth et al., 2005; Carcione, 2007). At low frequencies, the fluid has enough time to achieve pressure equilibration (relaxed regime). In this case, the Wood or Reuss model (Avseth et al., 2005) for the bulk modulus of the fluid mixture yields results that agree with the experiments. On the other hand, at high frequencies, the fluid can not relax, and this state of unrelaxation induces a stiffening of the pore material, which increases the wave velocity considerably. Here, we use a modified empirical fluid mixing law proposed by Brie et al. (1995), which gives the Wood modulus at low frequencies and the Voigt modulus at high frequencies (Avseth et al., 2005). This model is a good approximaton of the mesoscopic velocity dispersion based on the White theory (e.g., Carcione, 2007).

We consider the Bakken and Kimmeridge shales and calibrate the Backus and Gassmann models to the experimental data by calculating the seismic velocities as a function of kerogen. Then, we obtain the velocities as a function of oil and gas saturation, and frequency.

EFFECTIVE-MEDIA MODELS OF SEISMIC VELOCITY

We consider two models to obtain the velocities of the composite rock, namely, Backus averaging (Schoenberg and Muir, 1989) and Gassmann equations for a solid-pore infill (Ciz and Shapiro, 2007). The rock geometry corresponding to these models is shown schematically in Figure 1, where Figure 1a depicts the model used by Backus to represent a system of plane layers whose thicknesses are much smaller compared to the wavelength of the signal, Figure 1b shows a modification of the Backus model taking into account the discontinuity of the illite layers in the shale fabric, and Figure 1c is a representation of the shale based on Gassmann's assumptions to represent a porous medium. Regarding the model in Figure 1b, SEM observations have shown that the illite fabric has a lenticular pattern along the bedding plane rather a continuous-layer structure (Vernik and Nur, 1992). A reasonable way to model this effect is to substitute the bedding-plane elastic stiffnesses by a weighted average that takes into account the local proportion of illite and kerogen (see equation 15 below). On the other hand, Gassmann assumptions are that the wavelength is large compared with the dimensions of a macroscopic elementary volume. This volume has well-defined properties, such as porosity, permeability, and elastic moduli, which are representative of the medium. Scattering effects are thus neglected. Moreover, the liquid phase is continuous, and the matrix and pore space can have any shape, as shown in Figure 1c. The assumption of an anisotropic solid skeleton results from the alignment of the illite platelets (Sayers, 1999; Hornby et al., 1994)

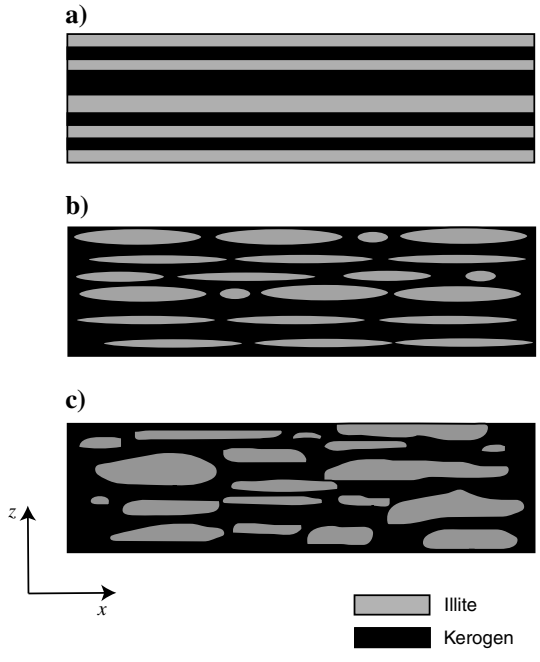

Figure 1. (a) Schematic fabric topology of transversely isotropic kerogen-rich shales, according to Backus model, (b) modified Backus model, and (c) Gassmann model. The z-direction corresponds to the symmetry axis.

We assume that the kerogen/oil/gas mixture consists of oil/gas bubbles embedded in a kerogen matrix and that the clay mineral is transversely isotropic. Calculation of the Gassmann moduli requires knowing the dry-rock elastic constants. These are obtained by a simple generalization of the Krief model (Krief at al., 1990). In the following, K and μ, and ρ indicate bulk and shear moduli, and density, and the indices m, s, o, g, f, k, and if denote dry matrix (skeleton), solid grain (clay), oil, gas, fluid (oil-gas mixture), kerogen and pore infill (oil-gas-kerogen mixture), respectively. Moreover, c_{IJ} is the two-indices notation for stiffnesses (Helbig, 1994) and ϕ denotes porosity or proportion of a given material.

Effective fluid model for partial gas saturation

The mixture oil/gas behaves as a composite fluid with properties depending on the constants of the constituents and their relative concentrations. The simplest solution is to assume Wood's average:

$$K_f = \left(\frac{S_g}{K_g} + \frac{S_o}{K_o}\right)^{-1} \tag{1}$$

and

$$\rho_f = S_g\rho_g + S_o\rho_o, \tag{2}$$

where S denotes saturation. Equation 1 corresponds to the low-frequency range. When the fluids are not mixed in the pore volume, but distributed in patches, the effective bulk modulus of the fluid at high frequencies is higher than that predicted by equation 1. We use an empirical mixing law introduced by Brie et al. (1995). The effective fluid bulk modulus is given by

$$K_f = (K_o - K_g)S_o^e + K_g, \tag{3}$$

where $e = (f_0/f)^{0.163}$ is an empirical parameter, with f the frequency and $f_0 = 1$ MHz being a reference frequency. Equation 3 gives Voigt's mixing law for $e = 1$ ($f = f_0$) and Wood's law for

$f = 25$ Hz. Equation 3 is consistent with White's mesoscopic model (White, 1975).

The gas density and bulk modulus as a function of pressure and temperature are calculated by using the van der Waals equation.

Properties of the kerogen/fluid mixture

The stiffnesses of the mixture can be calculated by using the model developed by Kuster and Toksöz (1974). If S is the fluid saturation, $S = \phi_f/(\phi_f + \phi_k)$, and the stiffnesses are

$$\frac{c_{13}^{if} + \frac{2}{3}c_{55}^{if}}{K_k} = \frac{1 + [4\mu_k(K_f - K_k)/(3K_f + 4\mu_k)K_k]S}{1 - [3(K_f - K_k)/(3K_f + 4\mu_k)]S} \quad (4)$$

and

$$\frac{c_{55}^{if}}{\mu_k} = \frac{(1 - S)(9K_f + 8\mu_k)}{9K_k + 8\mu_k + S(6K_k + 12\mu_k)}, \quad (5)$$

then the density of the mixture is simply $\rho_{if} = (\phi_k\rho_k + \phi_f\rho_f)/(\phi_k + \phi_f)$.

Dry-rock elastic constants

Gassmann's equation require the knowledge of the dry-rock elastic constants. Krief et al. (1990) proposed a simple heuristic equation:

$$K_m = K_s(1 - \phi)^{A/(1-\phi)} \quad \text{and} \quad \mu_m = K_m\mu_s/K_s, \quad (6)$$

where A is a constant which depends on the type of rock (the second expression in equation 6 is assumed here). The porosity dependence is consistent with the concept of critical porosity because the moduli should be small above a certain value of the porosity (usually between 0.4 and 0.6) (Mavko and Mukerji, 1998).

The properties of the skeleton can be described by an anisotropic version of the Krief model:

$$\begin{aligned} c_{11}^m &= c_{11}^s(1 - \phi)^{A/(1-\phi)}, \\ c_{66}^m &= c_{66}^s(1 - \phi)^{A/(1-\phi)}, \\ c_{13}^m &= c_{13}^s(1 - \phi)^{B/(1-\phi)}, \\ c_{33}^m &= c_{33}^s(1 - \phi)^{B/(1-\phi)}, \\ c_{55}^m &= c_{55}^s(1 - \phi)^{B/(1-\phi)}, \end{aligned} \quad (7)$$

where A and B are constants. The use of two constants is somehow equivalent to varying the Krief exponent as a function of the propagation (phase) angle because c_{11}^m and c_{66}^m describe the velocities along the stratification, and c_{33}^m and c_{55}^m along the perpendicular direction. As we shall see in the example, $A < B$, indicating that the critical porosity value is larger for the elastic constants describing the properties along the layering, i.e., the skeleton is mainly defined by these constants at high porosity. Equations 7 reduce to equation 6 for $A = B$ in the isotropic case.

Another possibility is to obtain the dry-rock elastic constants from wet-rock data by using the inverse Gassmann relation (see below).

Wet-rock Backus velocities

Following Vernik and Nur (1992) and Carcione (2000), we assume that the rock is a multilayer composite made of illite and kerogen (see Figure 1a and 1b). The Backus averaging gives a transversely isotropic equivalent medium described by five stiffnesses $\bar{c}_{IJ}$, where

$$\begin{aligned} \bar{c}_{11} &= \langle c_{11} - c_{13}^2c_{33}^{-1}\rangle + \langle c_{33}^{-1}\rangle^{-1}\langle c_{33}^{-1}\bar{c}_{13}\rangle^2 \\ \bar{c}_{33} &= \langle c_{33}^{-1}\rangle^{-1} \\ \bar{c}_{13} &= \langle c_{33}^{-1}\rangle^{-1}\langle c_{33}^{-1}c_{13}\rangle \\ \bar{c}_{55} &= \langle c_{55}^{-1}\rangle^{-1} \\ \bar{c}_{66} &= \langle c_{66}\rangle \end{aligned} \quad (8)$$

(Schoenberg and Muir, 1989; Carcione, 2007), with c_{IJ} the complex stifnesses corresponding to the single constituents, and $\langle\cdot\rangle$ indicating the weighted average. The proportion of the kerogen/oil/gas mixture is $\phi = \phi_k + \phi_f$ and the proportion of illite is $1 - \phi$.

The velocites are

$$\begin{aligned} v_{33} &= v_{\mathrm{P}}(0) = \sqrt{\bar{c}_{33}/\rho}, \\ v_{11} &= v_{\mathrm{P}}(90) = \sqrt{\bar{c}_{11}/\rho}, \\ v_{55} &= v_{\mathrm{S}}(0) = \sqrt{\bar{c}_{55}/\rho}, \\ v_{66} &= v_{\mathrm{S}}(90) = \sqrt{\bar{c}_{66}/\rho}. \end{aligned} \quad (9)$$

where subscripts P and S denote P- and S-waves, respectively, and 0 and 90 correspond to propagation perpendicular to and along the layering.

The bulk density is given by

$$\rho = (1 - \phi)\rho_s + \phi\rho_{if}. \quad (10)$$

Wet-rock Gassmann velocities

Ciz and Shapiro (2007) obtained the undrained compliance tensor when the pore infill and solid grains are anisotropic materials,

$$\begin{aligned} \bar{s}_{ijk\ell} = s_{ijk\ell}^m - (s_{ijmn}^m - s_{ijmn}^s)[\phi(\mathbf{s}^{if} - \mathbf{s}^{\phi}) + \mathbf{s}^m - \mathbf{s}^s]_{mnqp}^{-1} \\ \times (s_{qpk\ell}^m - s_{qpk\ell}^s), \end{aligned} \quad (11)$$

where the s's are the components of the compliance tensor, and the Einstein summation is assumed over 1, 2, and 3. Tensor and matrices are denoted with a bold font. The compliance tensor $\mathbf{s}^{\phi}$ is explicitly defined in Ciz and Shapiro (2007). In the case that the skeleton is made of a homogeneous material, $\mathbf{s}^{\phi} = \mathbf{s}^s$. Because the solid is transversely isotropic, we use the following relations between the Voigt stiffnesses and compliances: $c_{11} + c_{12} = s_{33}/s$, $c_{11} - c_{12} = 1/(s_{11} - s_{12})$, $c_{13} = -s_{13}/s$, $c_{33} = (s_{11} + s_{12})/s$, $c_{55} = 1/s_{55}$, where $s = s_{33}(s_{11} + s_{12}) - 2s_{13}^2$. The equations for the inversion are obtained by interchanging all the c and s values. Note the following relations: $s_{66} = 4s_{1212}$ and $s_{55} = 4s_{1313}$, valid for all the compliance tensors, whereas $c_{66} = c_{1212}$ and $c_{55} = c_{1313}$. The components of the corresponding undrained matrices transform in the same way. Moreover, the usual symmetry relations by interchanging the indices hold (e.g., Carcione, 2007).

In the limit of high porosities, say beyond 50%, the dry-rock elastic constants in equation 7 are zero in practice. In this limit, equation 11 becomes

$$\bar{s}_{ijk\ell} = (1-\phi)s^s_{ijk\ell} + \phi s^{if}_{ijk\ell}, \tag{12}$$

i.e., a generalization of the Reuss average.

Equation 11 can be inverted to obtain the dry-rock compliance tensor as a function of the undrained compliance tensor. We have

$$s^m_{ijk\ell} = s^s_{ijk\ell} + \phi(\bar{s}_{ijmn} - s^s_{ijmn})[\phi(\mathbf{s}^{if} - \mathbf{s}^{\phi}) - \bar{\mathbf{s}} + \mathbf{s}^s]^{-1}_{mnqp} \times (s^{if}_{qpk\ell} - s^{\phi}_{qpk\ell}). \tag{13}$$

This equation can be used to obtain the drained compliance tensor by using calibration data (seismic, well or laboratory data). Note that the Backus $\bar{c}_{55}$ and $\bar{c}_{66}$ in 8 are Reuss and Voigt averages, respectively. Hence, according to equation 12, the first stiffness is obtained from Gassmann's relations by assuming zero dry-rock stiffnesses. This means that an inversion of Backus generated stiffnesses by using equation 13 gives $c^m_{55} = 0$ because Backus's equation for $\bar{c}_{55}$ is a Reuss average as equation 12, that is satisfied when the dry-rock stiffness is zero.

EXAMPLES

Let us consider the data provided by Vernik and Nur (1992) in their Tables 1, 2 and 3 for the black shales of the Bakken formation, fully saturated with kerogen. We consider only the samples that have the P-wave velocity at 45° because this value is necessary to obtain c_{13}, and assume that the shales are transvesely isotropic. The wet-rock elastic constants are obtained as

$$\bar{c}_{33} = \rho v_P^2(0), \bar{c}_{11} = \rho v_P^2(90), \bar{c}_{55} = \rho v_S^2(0), \bar{c}_{66} = \rho v_S^2(90),$$
$$\bar{c}_{12} = 2\bar{c}_{66} - \bar{c}_{11}, \bar{c}_{13} = -\bar{c}_{55} + \sqrt{4\rho^2 v_P^4(45) - 2\rho v_P^2(45)(\bar{c}_{11} + \bar{c}_{33} + 2\bar{c}_{55}) + (\bar{c}_{11} + \bar{c}_{55})(\bar{c}_{33} + \bar{c}_{55})}, \tag{14}$$

(e.g., Carcione, 2007). Table 1 represents the data, together with the inverted dry-rock elastic constants (see below), the density and the kerogen content K. This is the volume fraction of kerogen in the rock and does not include the gas and oil bubbles. The material properties of the single media are given in Table 2, where v_{IJ} are the elastic velocities. The porosity of the Bakken shales is less than 1% and therefore we may assume that the rocks are made of illite and kerogen with no significant water saturation. The properties of illite and kerogen are those used by Vernik and Nur (1992), with the exception of the density of illite. We have assumed 2.6 g/cm^3 instead of 2.7 g/cm^3, which provides a better fit to the bulk density of the samples listed in Table 1 (see Figure 2). Figure 3 shows the Backus velocities (solid lines) as a function of kerogen content compared to the experimental data. The plots indicate that Backus averaging underestimates (at 0°) and overestimates (at 90°) the experimental velocities. This comparison suggests that the Backus velocities are suitable upper an lower limits. To obtain a better fit with the data, Vernik and Nur (1992) modify the elastic constants of illite, which has a lenticular textural pattern. They assume that only the stiffnesses "parallel to bedding" are affected:

$$c^s_{11} \to \langle c_{11} \rangle \quad \text{and} \quad c^s_{66} \to \langle c_{66} \rangle, \tag{15}$$

which incorporate the respective local constants of both illite and kerogen. The dashed curve in Figure 3 correspond to this modification of Backus averaging. The fit of the velocities parallel to layering has improved, but only for $v_S(90)$ is the match is acceptable.

On the other hand, Figure 4 shows the velocities versus kerogen content using Krief equations 7 with $\phi = K$ to calculate the dry-rock moduli (kerogen constitutes the pore-filling material), and Gassmann equation 11 to obtain the wet-rock moduli. We have used $A = 1.5$ and $B = 4$ in equation 7, as result of a visual best fit of the experimental data. The fit with the data is satisfactory.

The most realistic solution is to use equation 13, i.e., calculate the dry-rock moduli from the data. Table 1 shows the inversion using the properties given in Table 2 for illite and kerogen. The stability conditions for a transversely isotropic medium are

$$c_{11} > |c_{12}|, (c_{11} + c_{12})c_{33} > 2c^2_{13}, c_{55} > 0 \tag{16}$$

(e.g., Carcione, 2007). The wet media are all stable, while four out of eleven of the dry media are unstable, those at depths of 2630,

Table 1. Properties of the Bakken shales.

Depth (m)	$\bar{c}_{11}$(GPa)	$\bar{c}_{33}$(GPa)	$\bar{c}_{13}$(GPa)	$\bar{c}_{55}$(GPa)	$\bar{c}_{66}$(GPa)	c^m_{11}(GPa)	c^m_{33}(GPa)	c^m_{13}(GPa)	c^m_{55}(GPa)	c^m_{66}(GPa)	K	ρ(g/cm^{-3})
2630	30.7	21.9	12.0	9.6	10.6	21.9	9.3	12.5	6.3	7.2	0.44	1.99
2631	35.3	18.8	6.5	6.4	12.9	26.1	−5.3	0.6	−1.1	9.8	0.36	2.06
2996	38.2	25.7	9.6	9.5	11.8	27.5	2.4	7.2	1.8	5.7	0.25	2.21
3098	38.9	25.4	5.9	10.0	14.7	28.2	1.8	−2.1	4.0	11.5	0.27	2.22
3271	51.6	39.5	14.6	15.2	17.8	47.3	32.5	17.7	12.4	15.2	0.17	2.43
3271	46.9	27.9	11.4	9.2	16.0	42.9	11.7	12.1	1.8	13.6	0.26	2.33
3272	45.7	28.8	14.5	9.5	17.7	40.3	12.9	18.5	2.1	16.0	0.25	2.34
3332	51.2	25.4	15.8	8.1	17.6	47.5	−0.5	22.1	−2.8	15.8	0.24	2.35
3423	62.9	45.2	13.4	16.3	21.6	61.2	42.0	13.3	13.2	20.6	0.12	2.55
3428	45.2	32.9	9.9	12	16.0	38.8	20.0	8.7	6.7	12.7	0.21	2.38
3438	56.2	36.7	12.8	14.5	19.3	52.8	18.1	16.4	8.5	16.8	0.12	2.48

2631, 3272, and 3332 m. This may be due to several reasons: experimental errors, the shales are not exactly transversely isotropic, the properties of the kerogen and illite may vary from sample to sample and there may be free water saturation. In fact, some of the samples do not satisfy $v_{SV}(0) = v_{SV}(90)$ and some have a porosity between 1 and 2%. Actually, illite represents an assembly of more or less aligned clay particles that constitute a representative volume element of the clay component of the shale (in which case the hydration state can change) (see also the next section). Obviously, using these dry-rock moduli gives an "exact" match of the wet-rock data shown in Table 1, as there is a one-to-one mathematical correspondence between input and output values.

Three dynamic Poisson's ratios, corresponding to different directions can be obtained (e.g., Carcione and Cavallini, 2002): $\nu_1 = \epsilon_{yy}/\epsilon_{xx} = (c_{12}c_{33} - c_{13}^2)/(c_{11}c_{33} - c_{13}^2)$ and $\nu_2 = \epsilon_{zz}/\epsilon_{xx} = c_{13}(c_{11} - c_{12})/(c_{11}c_{33} - c_{13}^2)$, if the sample is compressed along the x-direction, and $\nu_3 = \epsilon_{xx}/\epsilon_{zz} = c_{13}/(c_{11} + c_{12})$, if the sample is compressed along the symmetry axis. Most of the dry-rock Poisson's ratio are positive, while $\nu_1 = -0.9$ (sample at 2996 m), $\nu_2 = -1$ and $\nu_3 = -0.06$ (sample at 3098 m), and $\nu_2 = -1.4$ (sample at 3332 m). Negative values have been reported by Mondol et al. (2007).

Let us consider the sample corresponding to a depth of 2631 m in Table 1, i.e., the symbols having $K = 0.36$ in Figure 4. Without any attempt to fit the velocities of this particular sample, we represent the energy velocity of the different modes in Figure 5, where the symbols correspond to the stiffnesses given in Table 1 for that sample and the solid lines to the Krief/Gassmann model shown in Figure 4. Because of the symmetry of the medium, only one-quarter of the polar plot is shown. (See the expression of the energy or group velocity in Carcione [2007], equations 1.148, 1.157, and 1.158.) The energy velocity of the SV wave has the characteristics of layered effective media. The wavefront is the energy velocity multiplied by 1 s. We have obtained the L_2-error of the stiffness $\rho v_P^2(45)$, summing up over all the samples in Table 1. The result is 10% and 5%, corresponding to the Backus and Gassmann models, respectively. As expected, a perfect fit for every sample at a given angle is not possible because the procedure is based on an average fit at two perpendicular directions, i.e., along the bedding plane and along the symmetry axis. Even at these two directions, the fit cannot be perfect due to experimental errors and possible deviations of the shale elastic symmetry from transverse isotropy.

A typical source rock in the North Sea source rocks is represented by the Kimmeridge shale from the Draupne Formation, with a maximum thickness of nearly 200 m, overlain by high-velocity chalk. The observed velocity contrast and thickness make the Kimmeridge an easily identified seismic unit. We report the elastic constants and properties of the single constituents in Tables 3 and 4, respectively. The samples considered here are those of Vernik (1995) at a confining pressure of 70 MPa. These samples have a porosity ranging from 5% to 20%, i.e., some parts of the shale are hydrated. The low velocities for illite in Table 4 take into account a fluid-softening effect by hydration of the smectite. Figure 6 shows the Backus velocities (solid lines) as a function of kerogen content compared to the experimental data. Part of the data, mainly $v_P(0)$ are outside the Backus bounds, but the trend is to satisfy Backus theoretical curves. The velocities versus kerogen content using the Krief/Gassmann

Table 2. Material properties of Bakken shales.

Medium	v_{11} (km/s)	v_{33} (km/s)	v_{55} (km/s)	v_{66} (km/s)	v_{13} (km/s)	$\rho(g/cm^{-3})$
Illite	5	4.5	2.9	3.15	1.96	2.6
Kerogen	2.7	2.7	1.5	1.5	1.7	1.4
Oil[a]	0.73	0.73	0	0	0.73	0.9
Gas[b]	0.32	0.32	0	0	0.32	0.1

[a]Oil/bitumen (McCain, 1984).
[b]Gas at 3-km depth.

Table 3. Properties of the Kimmeridge shales.

Depth (m)	$\bar{c}_{11}$(GPa)	$\bar{c}_{33}$(GPa)	$\bar{c}_{13}$(GPa)	$\bar{c}_{55}$(GPa)	$\bar{c}_{66}$(GPa)	K	$\rho(g/cm^{-3})$
2749	29.9	17.0	9.9	4.0	9.5	0.27	2.06
2768	31.9	18.9	6.0	5.5	9.1	0.4	2.22
2779	34.5	16.9	10.5	4.2	10.8	0.39	2.43
2818	40.9	28.1	15.4	7.9	14.1	0.16	2.33
2819	43.1	25.3	10.8	6.8	11.9	0.14	2.34
3574	37.8	23.6	13.7	6.6	12.1	0.24	2.35
3583	40.2	30.3	18.2	8.9	13.5	0.19	2.55
4449	48.4	34.5	14.9	9.8	14.7	0.13	2.38

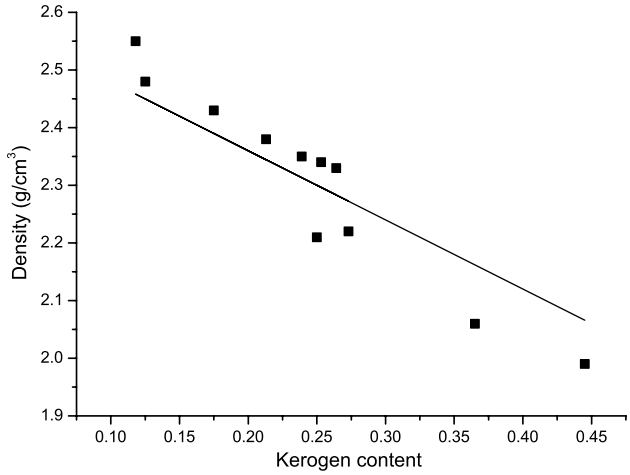

Figure 2. Bulk density as a function of kerogen content. The symbols correspond to the experimental data (Bakken shales) (Vernik and Nur, 1992).

equations are shown in Figure 7. We have used $A = 1.8$ and $B = 8$, with A assigned to c_{13} in equation 7. The fit with the data is satisfactory. The Gassmann inversion of the dry-rock moduli has not been successful for the Kimmeridge shale because seven samples do not satisfy the stability conditions. Because the inversion is based on average values of the properties of illite and kerogen (Table 4), a positive result is not guaranteed. Actually, each sample has different properties. In particular, the inverted c_{33}^m and c_{55}^m are very close to zero or are negative. Note that the Backus coefficients $\bar{c}_{33}$ and $\bar{c}_{55}$ in equation 8 are Reuss averages, respectively. According to equation 12, they can be obtained from Gassmann's relations by assuming zero dry-rock stiffnesses. This means that an inversion of Backus generated stiffnesses by using equation 13 gives $c_{33}^m = c_{55}^m = 0$.

Figure 8 shows the Krief/Gassmann wave velocities versus oil saturation for a Bakken shale with a porosity of 40%. The infill is a mixture of oil and kerogen. The P-wave velocity normal to the layering at 100% oil saturation is smaller than the S-wave velocity along the layering. (The medium satisfies the stability conditions 16 at all saturations.) The Gassmann velocities as a function of gas saturation at 25 Hz and 1 MHz are shown in Figure 9a and b, respectively. The porosity is 40% and the rock is saturated with 25% kerogen (a fixed amount) and 15% of an oil/gas mixture. With these proportions and the properties of gas at 3-km depth, there is no significant variation of the velocities as a function of gas saturation. In general, the velocities increase versus gas saturation due to the density effect, i.e., the density decreases with increasing gas saturation more rapidly than the elastic constants. The effect of frequency is also not very important for this particular case. In particular the S-wave velocities (along the pure-mode directions) do not depend on frequency, as expected for a Gassmann-type theory because the variations of K_f with frequency in equation 3 do not affect the shear stiffnesses. To see the dispersion effects, we plot in Figure 10 the percentage variation of the velocity between 1 MHz and 25 Hz versus gas saturation. The dispersion has a maximum at approximately 30% saturation and it is higher along the symmetry axis.

Finally, we represent the $v_P(0)/v_S(0)$ ratio as a function of gas saturation at 25 Hz (Figure 11). At $S_g = 0$ the shale is fully saturated with 40% kerogen, and gas, when present, forms bubbles in the kerogen material. The ratio is within the range expected for the Bakken shales (Ye, 2010) and decreases with increasing gas saturation.

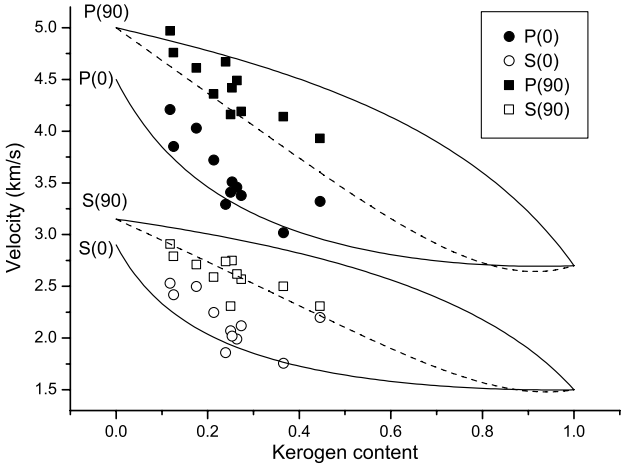

Figure 3. Backus velocities as a function of kerogen content. The symbols correspond to the experimental data (Bakken shales) (Vernik and Nur, 1992). The dashed line is the result of modifying the elastic constants of illite by assuming a lenticular textural pattern.

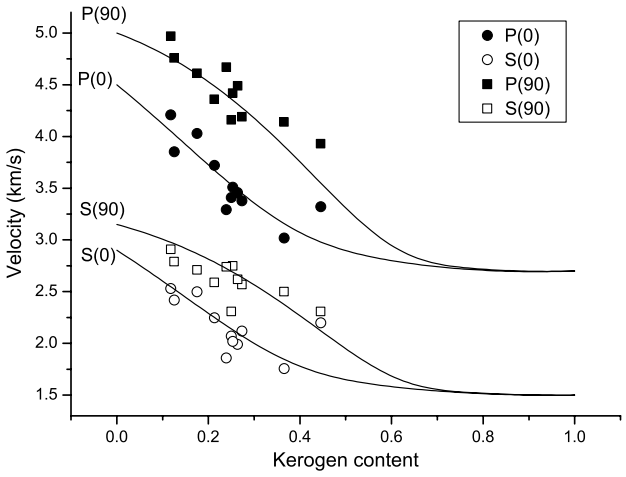

Figure 4. Gassmann velocities as a function of kerogen, where the dry-rock moduli have been obtained by a generalization of Krief equations to the anisotropic case. The symbols correspond to the experimental data (Bakken shales) (Vernik and Nur, 1992).

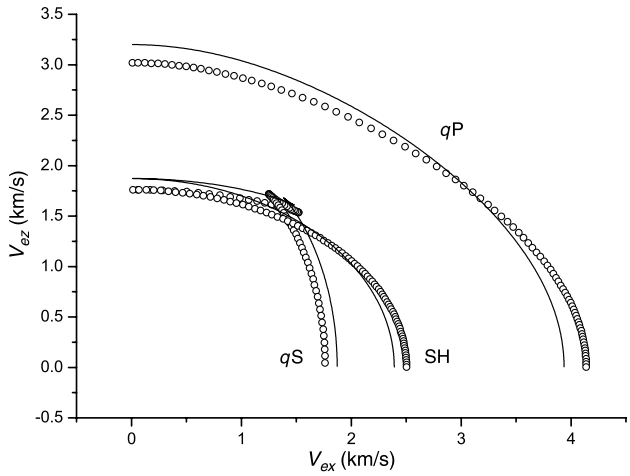

Figure 5. Polar representation of the energy velocity corresponding to the second sample in Table 1. The symbols correspond to the experimental data and the solid lines to Krief/Gassmann theory (Figure 4).

Table 4. Material properties of Kimmeridge shales.

Medium	v_{11} (km/s)	v_{33} (km/s)	v_{55} (km/s)	v_{66} (km/s)	v_{13} (km/s)	ρ(g/cm^3)
Illite	4.7	4.36	2.53	2.77	2.29	2.6
Kerogen	2.6	2.6	1.2	1.2	1.97	1.4

DISCUSSION

The methodology used here is based on models derived from physical principles (Kuster and Toksöz, Backus and Gassmann theories), and also on empirical relationships (Brie and Krief models). The limits of validity of the various laws and empirical models is discussed in the following.

The Kuster and Toksöz model does not account for inclusions (bubbles) interaction. The approximation is therefore valid only for dilute concentrations of inclusions. This limitation can be solved by adding the inclusions in small steps, such that the dilution criterion is satisfied. Despite this theoretical limitation, Nakagawa et al. (1995) have shown that in practice, the model with spherical inclusions match data reasonably well until at least 50% concentrations.

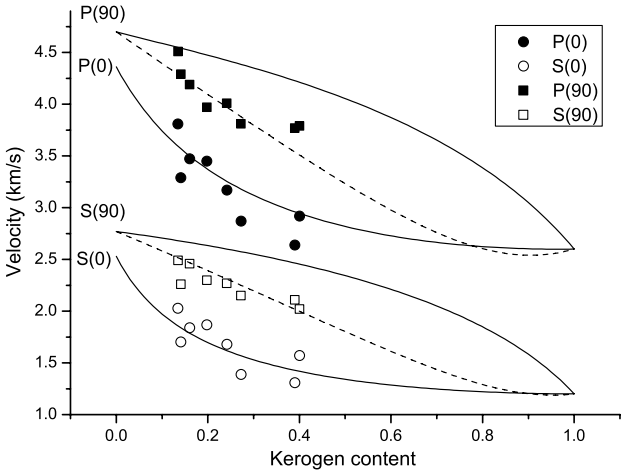

Figure 6. Backus velocities as a function of kerogen content. The symbols correspond to the experimental data (Kimmeridge shales) (Vernik, 1995). The dashed line is the result of modifying the elastic constants of illite by assuming a lenticular textural pattern.

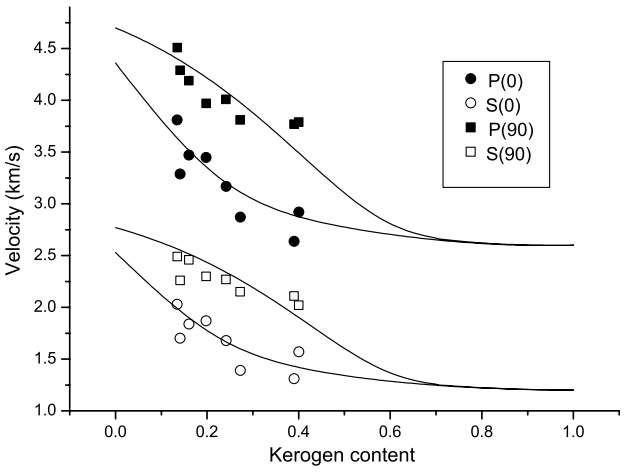

Figure 7. Gassmann velocities as a function of kerogen, where the dry-rock moduli have been obtained by a generalization of Krief equations to the anisotropic case. The symbols correspond to the experimental data (Kimmeridge shales) (Vernik, 1995).

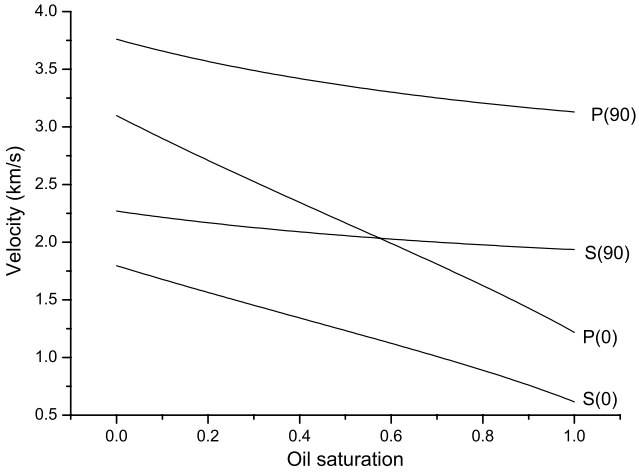

Figure 8. Gassmann velocities as a function of oil saturation. The porosity is 40% and the rock is saturated with kerogen and oil.

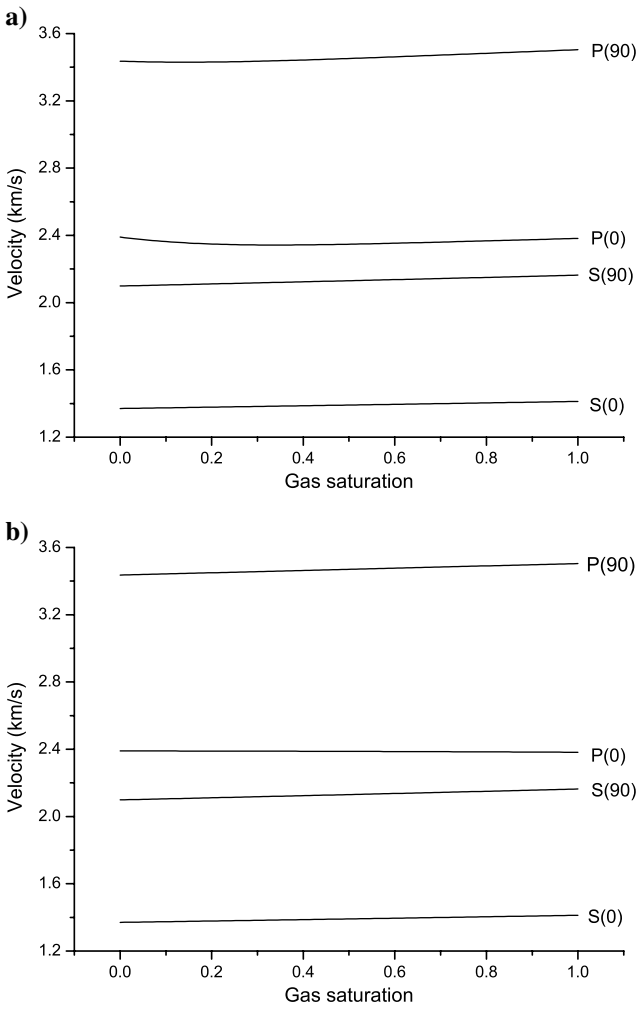

Figure 9. Gassmann velocities as a function of gas saturation at 25 Hz (a) and 1 MHz (b). The porosity is 40% and the rock is saturated with 25% kerogen and 15% of an oil/gas mixture.

Backus's theory is valid at low frequencies, i.e., when the dominant wavelength of the signal is much larger than the thickness of the layers composing the medium. Carcione et al. (1991) evaluated the long-wavelength approximation by using numerical modeling experiments. An acceptable rule of thumb is that the wavelength must be larger than eight times the layer thickness. Moreover, the theory holds for stationarity layering; that is, in a given length of the medium much smaller than the wavelength, the proportion of each material is constant (periodicity is not required).

The Krief model to obtain the dry-rock elastic constants is purely empirical and is equivalent to a critical-porosity model (Mavko and Mukerji, 1998). The anisotropic version (7) has two empirical parameters, A and B. The value used in the isotropic case is $A = 3$ (Mavko and Mukerji, 1998) and corresponds to the bulk and shear moduli. Here we have used values in the range [1,8] and this dispersion is due to the fact that the critical porosity value is larger for the elastic constants describing the properties along the layering, i.e., the rock matrix-stiffness is mainly described by these constants at high porosity.

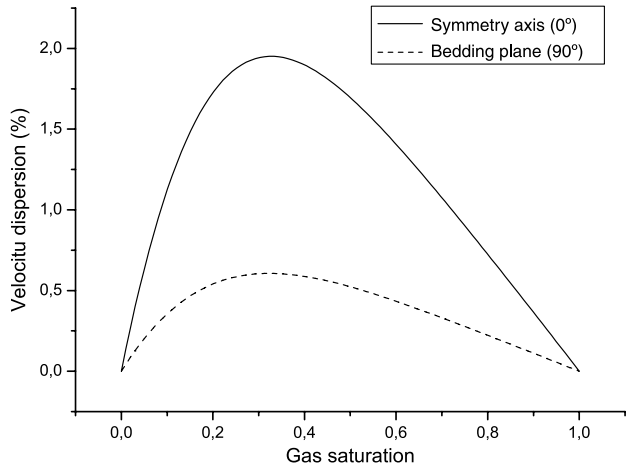

Figure 10. P-wave velocity dispersion along the symmetry axis (solid line) and along the layering plane (dashed line) as a function of gas saturation. The quantity represented is $[v_P(1\ \text{MHz}) - v_P(25\ \text{Hz})]/v_P(25\ \text{Hz})$.

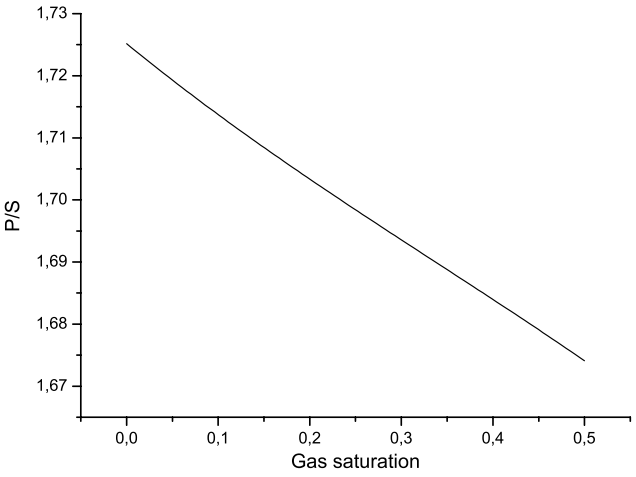

Figure 11. The ratio $v_P(0)/v_S(0)$ ratio as a function of gas saturation at 25 Hz. The porosity is 40% (kerogen content in the absence of gas).

Gassmann's relations are strictly valid at low frequencies, when the fluid has enough time to achieve pressure equilibration (relaxed regime). At high frequencies, the fluid cannot relax and this state of unrelaxation induces pore pressure gradients. Consequently, the rock is stiffer and the wet-rock moduli are higher than at low frequencies. This behavior can be described by the so-called mesoscopic-loss models, such as the one developed by White (1975). To overcome the low-frequency limitation, we use the Brie model to obtain an effective fluid bulk modulus at all frequencies. Equation (3) fits data from the seismic to the ultrasonic band, particularly, the sonic-band values provided by Brie et al. (1995). It gives Voigt's mixing law for $e = 1$ and an approximation to Wood's model for large e. The frequency dependence of this exponent describes the mentioned stiffening effect. The exponent e can be quantified on physical grounds by using White's model of patchy saturation (White, 1975). In this case, it can be assumed that the medium has patches of gas in an oil saturated background. An example is illustrated in Carcione et al. (2006).

Shale minerology may include kaolinite, montmorillonite-smectite, illite, and chlorite, so the term illite as used in this study may be representative for a mixture of clay minerals (Mondol et al., 2008). In the Kimmeridge clay, there is also some percentage of silty quartz (Williams et al., 2001). Moreover, as mentioned in the previous section, the illite layers represent an assembly of platelets, subject to internal hydration, so its mechanical properties such as the stiffnesses can vary depending on the source rock. The use of lower stiffnesses and 2.6 g/cm^3 as mineral density (as opposed to 2.7 g/cm^3 by Vernik and Nur, 1992) giving better fit to the data, may also indicate some intrinsic porosity in the illite layers. When modeling the effects of gas and oil generated from source rocks, we use effective porosity for the fluid substitution (see the difference between total and intrinsic porosity in Dvorkin et al., 2007).

A critical assumption when obtaining the properties of the pore-filing material could be that the oil and gas are present in spherical bubbles in the kerogen. Vernik (1994) has shown that there are microcracks within the kerogen or at kerogen-illite interfaces when the pore pressure exceeds the bedding-normal total stress by a few MPa. The conclusion that oil/gas saturation makes almost no difference at constant kerogen content could only be valid for spherical inclusions. The presence of gas from oil to gas conversion can open microcraks and change significantly the stiffness of the rock. Hence, an extension of this model to consider pore pressure and the presence of microcracks is needed.

An alternative model to Gassmann theory can be to consider kerogen part of the solid. A three-phase porous medium theory could be used, similar to that used by Carcione et al. (2000) and Gei and Carcione (2003) to obtain the acoustic properties of shaley sandstones and sediments saturated with clathrates, respectively. In this case, a generalization to the anisotropic case is required. A simpler model is to obtain the effective moduli of the solid component as the arithmetic average of the upper and lower Hashin-Shtrikman bounds and then use Brown and Korringa equations (e.g., Avseth et al., 2005).

CONCLUSIONS

Source rocks are described by using the Backus and the Krief/Gassmann models, assuming a transversely isotropic material

symmetry. Comparing the two models for Bakken shales indicates that the Backus model provides lower and upper bounds for the wave velocities, and that a suitable choice of parameters in the Krief model of the dry-rock elastic constants yields a good fit of the data by using Gassmann equations. The inverse Gassmann equations give exactly the dry-rock elastic constants for each sample. It is found that the dry medium is physically unstable in a few cases, i.e., the strain energy is not positive definite. This may due to several reasons, but mainly to the fact that the transversely isotropic symmetry can be a rough assumption for those cases. On the other hand, the velocities of the Kimmeridge shale are in agreement with Backus curves, and the Krief/Gassmann model also fits the data successfully. In the presence of fluids, such as oil and gas, the velocities vary considerably if the kerogen content varies, but they are relatively constant if the kerogen content is constant and the amount of gas and oil change.

ACKNOWLEDGMENTS

We thank Lundin Petroleum for partially funding the research, and Fabio Cavallini for helpful discussions. We also thank three anonymous reviewers and the associate editor for detailed comments.

REFERENCES

Avseth, P., T. Mukerji, and G. Mavko, 2005, Quantitative seismic interpretation: Cambridge University Press.

Brie, A., F. Pampuri, A. F. Marsala, and O. Meazza, 1995, Shear sonic interpretation in gas-bearing sands: SPE Annual Technical Conference, #30595, 701–710.

Carcione, J. M., 2000, A model for seismic velocity and attenuation in petroleum source rocks: Geophysics, **65**, 1080–1092, doi: 10.1190/1.1444801.

Carcione, J. M., 2007, Wave fields in real media: Theory and numerical simulation of wave propagation in anisotropic, anelastic, porous and electromagnetic media, 2nd edition, Elsevier Science.

Carcione, J. M., and F. Cavallini, 2002, Poisson's ratio at high pore pressure: Geophysical Prospecting, **50**, 97–106, doi: 10.1046/j.1365-2478.2002.00299.x.

Carcione, J. M., B. Gurevich, and F. Cavallini, 2000, A generalized Biot-Gassmann model for the acoustic properties of shaley sandstones: Geophysical Prospecting, **48**, 539–557, doi: 10.1046/j.1365-2478.2000.00198.x.

Carcione, J. M., D. Kosloff, and A. Behle, 1991, Long wave anisotropy in stratified media: A numerical test: Geophysics, **56**, 245–254, doi: 10.1190/1.1443037.

Carcione, J. M., S. Picotti, D. Gei, and G. Rossi, 2006, Physics and seismic modeling for monitoring CO2 storage: Pure and Applied Geophysics, **163**, 175–207, doi: 10.1007/s00024-005-0002-1.

Ciz, R., and S. Shapiro, 2007, Generalization of Gassmann equations for porous media saturated with a solid material: Geophysics, **72**, no. 6, A75–A79, doi: 10.1190/1.2772400.

Ciz, R., and S. Shapiro, 2009b, Stress-dependent anisotropy in transversely isotropic rocks: Comparison between theory and laboratory experiment on shale: Geophysics, **74**, no. 1, D7–D12 (See Erratum: Geophysics, **74**, no 6, Y5), doi: 10.1190/1.3008546.

Dvorkin, J., G. Mavko, and B. Gurevich, 2007, Fluid substitution in shaley sediment using effective porosity: Geophysics, **72**, no. 3, O1–O8, 10.1190/1.2565256.

Gei, D., and J. M. Carcione, 2003, Acoustic properties of sediments saturated with gas hydrate, free gas and water: Geophysical Prospecting, **51**, 141–158, 10.1046/j.1365-2478.2003.00359.x.

Helbig, K., 1994, Foundations of anisotropy for exploration seismics: Pergamon Press.

Hornby, B. E., L. M. Schwartz, and J. A. Hudson, 1994, Anisotropic effective medium modeling of the elastic properties of shales: Geophysics, **59**, 1570–1583, 10.1190/1.1443546.

Krief, M., J. Garat, J. Stellingwerff, and J. Ventre, 1990, A petrophysical interpretation using the velocities of P and S waves (full waveform sonic): The Log Analyst, **31**, no. 6, 355–369.

Kuster, G. T., and M. N. Toksöz, 1974, Velocity and attenuation of seismic waves in two-phase media: Part Theoretical I. Formulations: Geophysics, **39**, 587–606, 10.1190/1.1440450.

Mavko, G., and T. Mukerji, 1998, Comparison of the Krief and critical porosity models for prediction of porosity and V_P/V_S: Geophysics, doi: **63**, 925–927, 10.1190/1.1444403.

McCain, W. D., Jr., 1984, The properties of petroleum fluids: PennWell Books.

Mondol, N. H., K. Bjørlykke, J. Jahren, and K. Høeg, 2007, Experimental mechanical compaction of clay mineral aggregates — changes in physical properties of mudstones during burial: Marine and Petroleum Geology, **24**, 289–311, doi: 10.1016/j.marpetgeo.2007.03.006.

Mondol, N. H., J. Jahren, K. Bjørlykke, and I. Brevik, 2008, Elastic properties of clay minerals: The Leading Edge, 758–770, doi: 10.1190/1.2944163.

Nakagawa, S., N. G. W. Cook, K. T. Nihei, and L. R. Myer, 1995, Laboratory observation of seismic waves in heterogeneous geomaterials, *in* J. J. K., Daemen, and R. A. Schultz, eds., Proceedings of the 35th U.S. Symposium on Rock Mechanics: Balkema, 183–187.

Sarout, J., and Y. Guéguen, 2008, Anisotropy of elastic wave velocities in deformed shales: Part 2 — Modeling results: Geophysics, **73**, no. 5, D91–D103, doi: 10.1190/1.2952745.

Sayers, C. M., 1999, Stress-dependent seismic anisotropy of shales: Geophysics, **64**, 93–98, doi: 10.1190/1.1444535.

Schoenberg, M., and F. Muir, 1989, A calculus for finely layered media: Geophysics, **54**, 582–590, doi: 10.1190/1.1442685.

Sondergeld, C. H., R. J. Ambrose, C. S. Rai, and J. Moncrieff, 2010, Micro-structural studies of gas shales: SPE 131771, Proceedings of SPE Unconventional Gas Conference, **2**, 3–25.

Vernik, L., 1994, Hydrocarbon-generation-induced microcracking of source rocks: Geophysics, **59**, 555–563, doi: 10.1190/1.1443616.

Vernik, L., 1995, Petrophysics of the Kimmeridge shale, North Sea: Stanford Rock Physics Laboratory.

Vernik, L., and A. Nur, 1992, Ultrasonic velocity and anisotropy of hydrocarbon source rocks: Geophysics, **57**, 727–735, doi: 10.1190/1.1443286.

White, J. E., 1975, Computed seismic speeds and attenuation in rocks with partial gas saturation: Geophysics, **40**, 224–232, doi: 10.1190/1.1440520.

Williams, C. J., S. P. Hesselbo, H. C. Jenkyns, and H. S. Morgans-Bell, 2001, Quartz silt in mudrocks as a key to sequence stratigraphy (Kimmeridge Clay Formation, Late Jurrasic, Wessex Basin, UK): Terra Nova, **13**, 449–455, doi: 10.1046/j.1365-3121.2001.00378.x.

Ye, F., 2010, Sensitivity of seismic reflections to variations in anisotropy in the Bakken formation, Williston Basin, North Dakota, The University of Texas at Austin, M.S. thesis.